JOURNAL OF AIRCRAFT
Vol. 39, No. 2, March–April 2002

Optimal Short Takeoff of Tiltrotor Aircraft in One Engine Failure

Eric B. Carlson*
Bell Helicopter Textron, Fort Worth, Texas 76101
and
Yiyuan J. Zhao†
University of Minnesota, Minneapolis, Minnesota 55455

Optimal tiltrotor flight paths in the event of a single engine failure during short takeoff operations are investigated. A vertical plane rigid-body model is used that has as state variables aircraft position, body components of aircraft velocity, pitch angle and rate, and rotor angular speed. The control variables are the thrust coefficient of one rotor, the pilot's longitudinal stick displacement, and the nacelle angle. The model uses both parameters and aerodynamic data of the XV-15 research aircraft. The tabular aerodynamic data are interpolated with smooth functions. Tiltrotor flights after engine failure are formulated as nonlinear optimal control problems. Both continued takeoff and rejected takeoff flight after an engine failure are studied. Performance indices are selected to minimize runway length, subject to various constraints from safety considerations and tiltrotor performance limitations. These optimal control problems are parameterized via collocation into parameter optimizations for numerical solutions. Extensive numerical solutions are obtained, and sensitivity analyses are conducted to examine effects of model uncertainties.

Nomenclature

A_x = x component of aerodynamic force in body reference frame
A_z = z component of aerodynamic force in body reference frame
a = acceleration
C_P = required power coefficient
C_T = single rotor thrust coefficient
c_d = average rotor blade drag coefficient
c_w = mean wing chord, ft
D = drag, lb
d = distance between nacelle rotation point and hub center
f_G = ground effect factor
g = acceleration due to gravity, ft/s^2
h = tiltrotor altitude, ft
h_R = above c.g. location of nacelle rotation point
I_R = rotor polar moment of inertia, slugs $\cdot$ ft^2
I_y = pitch moment of inertia slugs $\cdot$ ft^2
i_n = nacelle angle, rad
K_{ind} = induced power factor, >1
K_Ω = rotor speed feedback control gain
L = lift, lb
l_R = behind c.g. location of nacelle rotation point
M = total aerodynamic pitching moment, lb $\cdot$ ft
$\mathcal{M}$ = Mach number
m = tiltrotor mass
P_{AEO} = all engine operating power rating
P_a = power available, ft $\cdot$ lb/s
P_{OEI} = one engine power rating when the other engine is inoperative
P_r = power required, ft $\cdot$ lb/s
q = pitch rate, rad/s, dynamic pressure (with subscript)
R = rotor radius, ft
S = a generic reference area, ft^2
S_{hs} = horizontal stabilizer platform area
S_w = wing platform area
$S_{w_{\text{fs}}}$ = wing area in freestream
$S_{w_{\text{ss}}}$ = wing area in rotor slip stream
s = longitudinal stick displacement, in.
T = thrust from one rotor, lb
t_d = pilot delay time, s
t_p = power available time constant, s
U_c = flow perpendicular to rotor plane, ft/s
U_t = flow parallel to rotor plane, ft/s
u = horizontal velocity component in body axes, ft/s
V = airspeed
V_L = liftoff speed on short takeoff
v_i = induced velocity, ft/s
W = gross weight, lb
w = vertical velocity component in body reference frame, ft/s, positive down
x = horizontal location of aircraft
α = angle of attack, rad
β = cyclic angle, rad
γ = flight-path angle
δ_e = elevator deflection, rad
δ_{fl} = flap angle
η_h = horizontal stabilizer flow reduction factor
η_i = rotor induced velocity development factor
η_p = power consumption correction factor
θ = pitch angle, rad
μ = advance ratio
ρ = air density, slugs/ft^3
σ = rotor solidity ratio
Ω = rotor speed, rad/s
Ω_0 = nominal rotor speed

Superscripts

$\dot{}$ = time derivative
$'$ = derivative with respect to normalized time
$\bar{}$ = normalized variable

Received 5 October 2000; revision received 1 August 2001; accepted for publication 21 August 2001.

*Senior Engineer, Aerodynamics, P.O. Box 482.
†Associate Professor, Aerospace Engineering and Mechanics. Senior Member AIAA.

I. Introduction

TILTROTOR aircraft combine the advantages of helicopters in low-speed flight and turboprop airplanes in high-speed flight

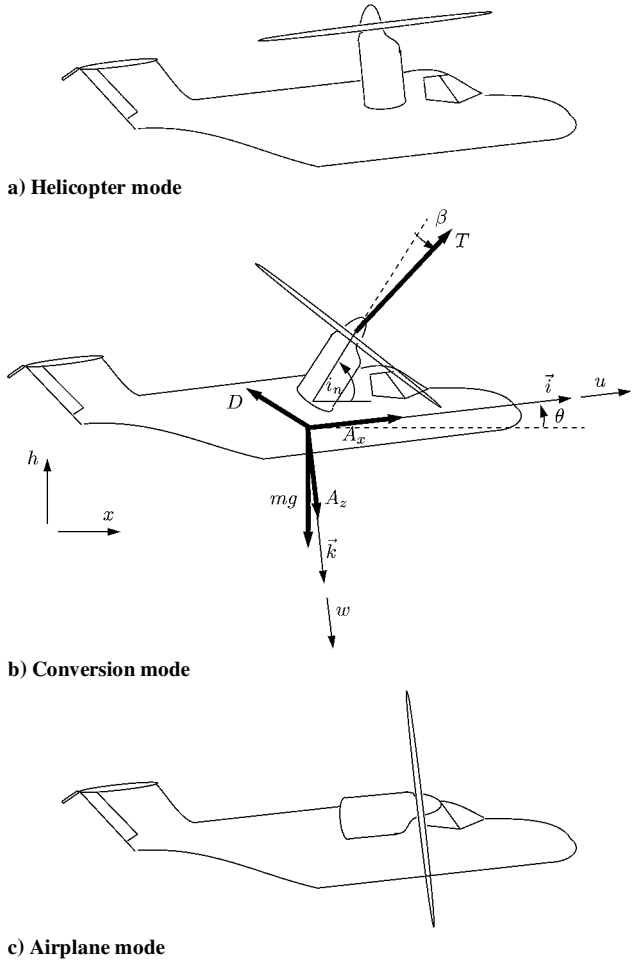

Fig. 1 Tiltrotor in its three modes of flight.

(Fig. 1). Their two proprotors, located at the tips of their wings, can tilt from a vertical orientation (helicopter mode) to a horizontal orientation (airplane mode). They act as rotors in helicopter mode, providing both lift and thrust. As the aircraft converts into the airplane mode with increasing speed, both lift generation and attitude control are transfered from the proprotors to the classical airplane wing and control surfaces. The proprotors then act as classical airplane propellers. The ability to fly both as a helicopter and as an airplane allows tiltrotor aircraft to utilize some of the best aspects of both types of flight.[1–6]

The U.S. government, in conjunction with industry, has been designing and testing tiltrotor aircraft for over 40 years. The Bell Helicopter Textron XV-3 convertiplane was the tiltrotor prototype tested in the 1950s and 1960s. It showed that tiltrotor aircraft could be advantageous in many applications. Next came the Bell XV-15 tiltrotor research aircraft of the 1970s, which demonstrated that all of the major limitations of the XV-3 could be overcome.[1] Then the V-22 Osprey was designed and built by Bell Helicopter Textron and The Boeing Company.[6] The bigger V-22 is a culmination of 30 years of research and is currently being built for military use. Recently, Bell Helicopter Textron (now in conjunction with Agusta) announced its plan to build a commercial tiltrotor aircraft. The 609 is proposed as a six to nine passenger tiltrotor (similar in size and design to the XV-15) with a maximum cruise speed of 275 kn and a maximum range of 750 n mile.

Engine failure during takeoff and landing poses a serious threat to safe tiltrotor operations. As a result, tiltrotor aircraft must demonstrate satisfactory flight characteristics in the event of an engine failure, to win the certification from the Federal Aviation Administration (FAA). It is expected that the certification standards for civil tiltrotor aircraft will be similar or identical to those for category-A helicopter. The category-A helicopter certification applies to helicopter with more than one independent engine systems.[7] It requires that, in the event of a single engine failure, the helicopter must be able to either continue the flight or land safely, depending on the helicopter conditions at engine failure and available airport dimensions. In particular, the point on a nominal takeoff path at which the decision is made whether to continue or to reject the flight in case of one engine failure is called the takeoff decision point. In the certification process of an individual rotorcraft, performance questions that must be answered include maximum gross weight capabilities, runway requirements, decision point conditions, and proper flight strategies in engine failure.

Theoretical analyses have been used to study tiltrotor flights in engine failure. In Ref. 5, rate of descent in engine failure was calculated for a range of airspeeds, and flare procedures were discussed. In Refs. 8 and 9, Okuno and Kawachi applied nonlinear optimal control theories and compared different modes of tiltrotor takeoff flight in engine failures. Cerbe et al. used parameter optimization methods and studied optimal short takeoff flight paths of a tiltrotor aircraft in the event of one engine failure.[10] Pollack et al.[11] conducted simulation studies to examine vertical takeoff procedures for tiltrotor aircraft. Warburton and Curtiss[12] evaluated a tiltrotor aircraft design by using real time interactive simulations. Carlson et al. investigated flight procedures and performance limits of tiltrotor aircraft in total power failure.[13] Recently, Carlson[14] conducted extensive optimization studies of tiltrotor aircraft flight procedures and performance limits in one engine failure.

This paper examines optimal short takeoff procedures of a tiltrotor aircraft considering the possibility of one engine failure. Optimal control theories are used to obtain insights into maximum gross weight capabilities, runway length requirements, decision point conditions, and flight strategies in engine failure for a tiltrotor aircraft on a short takeoff flight.

Studies of tiltrotor flights have several special challenges compared to those for conventional helicopters.[15–21] In particular, a comprehensive longitudinal tiltrotor model must represent forces and moments produced by the rotors, the wing, and the elevator. This is important because the pilot stick control affects both rotor thrust inclination and elevator deflection. Because a tiltrotor can fly like a helicopter, forces and moments for all aerodynamic surfaces and the fuselage must be modeled for the full range of angle of attack. Finally, that part of the wing is in the slip stream of the rotors and, thus, experiences a download effect, which must be included in the model.

In this paper, a vertical plane rigid-body model for tiltrotor aircraft is first developed. Full-range aerodynamic data for the XV-15 are interpolated with smooth functions. Download on the wing is modeled by considering the parts of the wing in the freestream and slip stream separately. Flights after one engine failure during a short takeoff operation are formulated as nonlinear optimal control problems. Realistic constraints are imposed from safety requirements and tiltrotor performance limitations. Numerical methods are used to determine solutions of these optimal control problems.

This paper presents selected results of the work in Ref. 14. See Ref. 14 for further details.

II. Tiltrotor Aircraft Modeling

A vertical plane rigid-body model of a tiltrotor aircraft representative of the XV-15 is derived by Carlson[14] and is repeated here for convenience (Fig. 1b):

$$\dot{w} = (1/m)[A_z - 2T\sin(i_n - \beta)] + g\cos\theta + qu \tag{1}$$

$$\dot{u} = (1/m)[A_x + 2T\cos(i_n - \beta)] - g\sin\theta - qw \tag{2}$$

$$\dot{\theta} = q \tag{3}$$

$$\dot{q} = (1/I_y)\{M - 2T[l_R\sin(i_n - \beta) + h_R\cos(i_n - \beta) + d\sin\beta]\} \tag{4}$$

$$\dot{\Omega} = (1/I_R)[(P_a - P_r)/\Omega] \tag{5}$$

$$\dot{h} = u\sin\theta - w\cos\theta \tag{6}$$

$$\dot{x} = u\cos\theta + w\sin\theta \tag{7}$$

In these equations, the state variables are $[w, u, \theta, q, \Omega, h, x]$ and control variables are $[T, s, i_n]$. Airspeed and flight-path angle can be determined from

$$V = \sqrt{u^2 + w^2} \tag{8}$$

$$\gamma = -\sin^{-1}(w/V), \qquad V \neq 0 \tag{9}$$

For the XV-15, the pilot's longitudinal stick displacement affects both the rotor cyclic and the elevator deflection angle. The elevator remains active during all modes of tiltrotor flight but is ineffective at low speeds. The rotor cyclic is, therefore, the effective control of attitude in helicopter mode ($i_n = 90$ deg), but it is phased out as the nacelle angle is rotated down to airplane mode ($i_n = 0$). Mathematically,

$$\beta = \beta_{\max}(s/s_{\max})\sin i_n \tag{10}$$

$$\delta_e = \delta_{e_{\max}}(s/s_{\max}) \tag{11}$$

where Eq. (10) represents an approximation to Fig. 13 in Ref. 4.

A. Rotor-Induced Velocity

Rotor-induced velocity v_i is needed to determine aerodynamic forces and moments and the power required. Define

$$U_c = (u - qh_R)\cos(i_n - \beta) - (w + ql_R)\sin(i_n - \beta) - qd\sin\beta \tag{12}$$

$$U_t = (u - qh_R)\sin(i_n - \beta) + (w + ql_R)\cos(i_n - \beta) - qd\cos\beta \tag{13}$$

Normalize U_c, U_t, and v_i by the mean induced velocity at hover v_h

$$\bar{U}_c = U_c/v_h, \qquad \bar{U}_t = U_t/v_h, \qquad \bar{v}_i = v_i/v_h \tag{14}$$

where

$$v_h = \sqrt{T/2\rho\pi R^2} \tag{15}$$

For rotor flows outside the vortex-ring state, $(2\bar{U}_c + 3)^2 + \bar{U}_t^2 > 1$, the normalized ideal induced velocity can be determined from the momentum theory,[22–24]

$$\bar{v}_i^4 + 2\bar{U}_c\bar{v}_i^3 + \left(\bar{U}_c^2 + \bar{U}_t^2\right)\bar{v}_i^2 = 1 \tag{16}$$

Inside the vortex-ring state, $(2\bar{U}_c + 3)^2 + \bar{U}_t^2 \leq 1$, the induced velocity can be determined from an approximation proposed by Johnson[15]:

$$\bar{v}_i = \bar{U}_c\left(0.373\bar{U}_c^2 + 0.598\bar{U}_t^2 - 1.991\right) \tag{17}$$

B. Power Available and Power Required

When an engine failure occurs, the power available from the failing engine decreases from the normal all engine operating (AEO) rating to zero, whereas the working engine increases its power to the one engine inoperation (OEI) power rating. Power available is, therefore, a function of time and can be described by

$$P_a = (P_{\text{AEO}} - P_{\text{OEI}})e^{-t/t_p} + P_{\text{OEI}} \tag{18}$$

The total power required to drag the rotors through the air is

$$P_r = (2/\eta_p)\rho(\pi R^2)(\Omega R)^3 C_P \tag{19}$$

where

$$C_P = C_T\sqrt{C_T/2}(K_{\text{ind}}f_G\bar{v}_i + \bar{U}_c) + \tfrac{1}{8}\sigma c_d(1 + 4.7\mu^2) \tag{20}$$

$$C_T = T/\rho(\pi R^2)(\Omega R)^2 \tag{21}$$

$$\mu = U_t/\Omega R \tag{22}$$

C. Aerodynamic Forces and Moments

The total aerodynamic force and moment are taken from the fuselage, wing–pylons, and the horizontal stabilizer–elevator system. In particular, aerodynamic forces and moments of the wing consist of those from the part of the wing inside the rotor slip stream and the part of the wing in the freestream. Expressions of aerodynamic forces and moments are provided in Appendix A, whereas functional dependences of these forces are given hereafter for the completeness of equations of motion:

$$A_z = A_z(w, u, q, \Omega, T, s, i_n; \delta_{\text{fl}}, \mathcal{M}) \tag{23}$$

$$A_x = A_x(w, u, q, \Omega, T, s, i_n; \delta_{\text{fl}}, \mathcal{M}) \tag{24}$$

$$M = M(w, u, q, \Omega, T, s, i_n; \delta_{\text{fl}}, \mathcal{M}) \tag{25}$$

Aerodynamic coefficients for the XV-15 are given in tabular forms,[25] for the full angle-of-attack range (from -180 to 180 deg), different nacelle angles (from 0 to 95 deg), different flap angles (0, 20, 40, and 75 deg), and different Mach numbers. For the efficiency of optimization studies, these data are interpolated into smooth functions. Cubic spline polynomial interpolations and in some cases least-squares fits are used. Details are reported by Carlson.[14]

Parameters used in the optimization studies are given in Appendix B.

D. Normalization and Scaling

Proper normalization and scaling of all variables used in numerical optimizations can help the convergence of an optimization algorithm. The following normalizations and scalings are used for the current study:

$$\bar{w} = \frac{100w}{\Omega_0 R}, \qquad \bar{u} = \frac{100u}{\Omega_0 R}, \qquad \bar{q} = \frac{100q}{\Omega_0}, \qquad \bar{\theta} = \theta \tag{26}$$

$$\bar{\Omega} = \frac{\Omega}{\Omega_0}, \qquad \bar{h} = \frac{h}{R}, \qquad \bar{x} = \frac{x}{R} \tag{27}$$

$$\tau = 0.01\Omega_0 t \Rightarrow \frac{\mathrm{d}(\,)}{\mathrm{d}\tau} = \frac{100}{\Omega_0}\dot{(\,)} \tag{28}$$

and

$$\bar{C}_T \triangleq 10^4(2\rho\pi R^3/m)C_T \tag{29}$$

$$\bar{s} \triangleq s/s_{\max} \tag{30}$$

E. Steady-State Analysis and Model Validation

The steady-state tiltrotor flight conditions satisfy Eqs. (1–5) with $\dot{w}$, $\dot{u}$, $\dot{\theta}$, $\dot{q}$, and $\dot{\Omega}$ all equaling zero. For some specified states and/or controls, these steady-state equations can be used to determine values of remaining states and/or controls. In this paper, a Newton–Raphson scheme is used to solve these equations numerically. Steady-state analysis can be used to generate power required data at steady states for which flight-test data are available.[25] In Ref. 14, calculated steady-state power requirements from the preceding vertical plane rigid-body model show good agreements with flight-test power requirement data over the speed range of takeoff flight.

In addition, augmented steady-state equations are solved to produce initial conditions for the optimization studies. In doing so, the steady-state equations are modified by including constant acceleration terms.

III. Problem Statement

The unique design of a tiltrotor aircraft allows it to take off in ways different from other aircraft. In a runway takeoff, a tiltrotor would accelerate along a runway with a forward nacelle tilt of 15–30 deg. At a certain speed, where the power required is low enough, the vertical lift and thrust will surpass the weight and the climbout can begin. If only an open field is available, a tiltrotor can accelerate

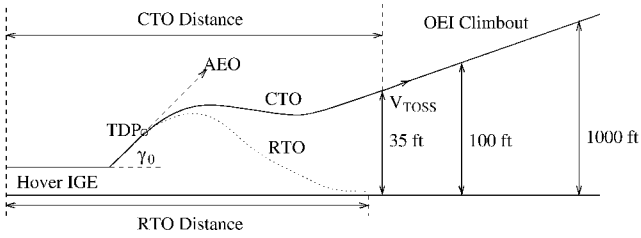

Fig. 2 Category-A helicopter short takeoff operation.

forward in ground effect close to the ground, with either a forward nacelle or a negative pitch. Both of these procedures are short takeoff procedures. Sometimes, for terminology convenience, the first will be referred to as a runway takeoff and the second a short takeoff. In confined areas, a tiltrotor can take off vertically. Specific vertical takeoff procedures depend on characteristics of the heliport. Finally, oblique takeoff procedures are somewhere between the short takeoff procedure and the vertical takeoff procedure and can be used when the takeoff area is somewhat confined.

When the aircraft has gained enough height and speed for safety, the nacelle conversion process can begin to reap the efficiencies of airplane flight. A conversion technique developed by the XV-15 tiltrotor test pilots[2] would accelerate the tiltrotor forward to a speed of 60–80 kn by tilting the nacelle forward from 10 to 20 deg from their vertical orientation. At this speed, a continuous conversion is possible at a maximum of 7.5 deg of tilt per second. As this transition is taking place, the rotor controls are mechanically phased out and control is taken over by the airplane control surfaces. Once the rotors have been tilted completely forward, they are held fixed to the wing. The pilot then reduces the rotor speed to the airplane mode setting to increase efficiency and reduce vibrations. This conversion process can be safely aborted at any time, and the tiltrotor can fly at any possible nacelle angle in its range from 0 to 95 deg. The reconversion process is the identical procedure in reverse. The rotors' angular velocity is first increased back to the helicopter/conversion mode setting and the forward speed is decreased by reducing the power. A continuous reconversion can then be accomplished at the 7.5 deg/s tilt or a slower rate. During this process, the tiltrotor continues to decelerate. Once converted, the tiltrotor can execute the landing procedure appropriate to the area. It can touch down softly like a helicopter or roll onto a runway. At touchdown, the nacelle can be at any angle that keeps the rotor tips a sufficient clearance from the ground (for the XV-15, this is 60–95 deg).

Tiltrotor aircraft must demonstrate satisfactory flight performances in the event of an engine failure. Because of their vertical takeoff and landing capability, the FAA will require civil tiltrotor aircraft to be certified in a fashion similar or identical to category-A helicopter.[7] This requires specific procedures during takeoff and landing to maintain the highest degree of safety in case an engine failure occurs. Specifically, during a short takeoff (Fig. 2), the pilot must reject the takeoff [rejected takeoff (RTO)] if an engine failure occurs before the takeoff decision point (TDP). The takeoff must be continued [continued takeoff (CTO)] if an engine fails after the TDP. At the end of the transient CTO flight, the aircraft must achieve a steady OEI climb with specified conditions.

Flight manual instructions for a tiltrotor aircraft must specify TDP conditions and appropriate flight strategies for CTO and RTO flights. These conditions and recommendations depend on the weight of the aircraft, the usable runway field length, and ambient conditions. Conversely, choices of TDP conditions and flight strategies in OEI affect the gross weight capabilities and runway length requirements.

The problems in this paper are to determine optimal TDP conditions, gross weight capabilities, and runway lengths required during a short takeoff operation considering the possibility of one engine failure, as well as main characteristics of optimal CTO and RTO flights in OEI.

IV. Formulations of Optimal Control Problems

Formulations of optimal control problems refer to the selections of performance indices and constraints. There are three important concerns for tiltrotor flights in OEI: safety, gross weight capability, and runway field length. The basic safety requirements are specified in the FAA certification regulations. To study the gross weight capabilities and runway length requirements in OEI, both CTO and RTO need to be examined. In general, there is a tradeoff between gross weight capability and runway length requirement. One can either maximize the gross weight for a specified runway length or minimize the runway length required while systematically varying the gross weight. The second approach is used here.

The following path constraints are imposed in all optimization studies in this paper to make tiltrotor flights physically meaningful. Path constraints on state variables include

$$\theta_{\max} \geq \theta \geq \theta_{\min}, \qquad \Omega_{\max} \geq \Omega \geq \Omega_{\min}, \qquad h \geq h_{\min} \tag{31}$$

and path constraints on control variables include

$$C_{T_{\max}} \geq C_T \geq C_{T_{\min}}, \qquad s_{\max} \geq s \geq -s_{\max}$$
$$i_{n,\max} \geq i_n \geq i_{n,\min} \tag{32}$$

In addition, use of the finite state approximation to the optimal control problems formulated hereafter allow one to impose constraints on control rates

$$|\dot{C}_T| \leq \dot{C}_{T_{\max}}, \qquad |\dot{s}(t)| \leq \dot{s}_{\max}, \qquad |\dot{i}_n| \leq \dot{i}_{n_{\max}} \tag{33}$$

A. CTO in OEI

For CTO, a safe OEI climbout is defined by a final height of at least 35 ft, a final climb rate of at least 100 ft/min, and a sustainable steady-state flight. A sustainable steady-state climbout requires the tiltrotor aircraft to achieve a minimum forward speed of V_{TOSS}, known as the takeoff safety speed (TOSS) at the end of the transient CTO flight. This is the speed that allows for a steady-state climbout at a given weight with the available power P_{OEI}. In the current paper, this steady-state speed is automatically satisfied by the steady-state requirements in Eqs. (37–41).

An optimal control problem is formulated to minimize the runway length required during the transient CTO flight from the point of engine failure to the establishment of a safe OEI climbout (Fig. 2). Mathematically,

$$\min x(t_f) \tag{34}$$

subject to Eqs. (1–7), the path constraints in Eqs. (31–33), and the following terminal constraints:

$$h(t_f) \geq 35\,\text{ft} \tag{35}$$

$$\dot{h}(t_f) \geq 100\,\text{fpm} \tag{36}$$

$$\dot{w}(t_f) = 0 \tag{37}$$

$$\dot{u}(t_f) = 0 \tag{38}$$

$$\dot{\theta}(t_f) = 0 \tag{39}$$

$$\dot{q}(t_f) = 0 \tag{40}$$

$$\dot{\Omega}(t_f) \geq 0 \tag{41}$$

In most flight conditions, these inequality constraints become equalities on optimal solutions.

B. RTO in OEI

For RTO flight in OEI, the problem is to minimize the required runway length

$$\min\ x(t_f) + \left[\dot{x}^2(t_f)/2a\right] \tag{42}$$

subject to Eqs. (1–7), the path constraints in Eqs. (31–33), and the following terminal constraints:

$$h(t_f) = 0 \tag{43}$$

$$\dot{x}(t_f) \le \dot{x}_{f,\max} \tag{44}$$

$$\dot{h}(t_f) \le \dot{h}_{f,\max} \tag{45}$$

$$\theta_{f,\min} \le \theta(t_f) \le \theta_{f,\max} \tag{46}$$

$$i_n(t_f) \ge i_{n_{f,\min}} \tag{47}$$

where Eqs. (44–47) specify a safe touchdown condition, and the second part in Eq. (42) accounts for the ground distance needed for the tiltrotor to stop. It is assumed that $a = 0.2\,g$ here.

The constraint in Eq. (47) is imposed to limit the nacelle tilt angle to avoid rotor ground strike. The direct inclusion of this inequality constraint is possible only in the finite dimensional numerical approximation to this problem. Strictly speaking, the time rate of i_n needs to be treated as a control variable for Eq. (47) to be meaningful in an infinite dimensional optimal control problem.

C. Numerical Solution Methods

The optimal control problems just formulated are solved numerically with a collocation approach,[26–28] in which both state and control variables are parameterized. Differential equations are enforced as a system of nonlinear constraints through a forward difference approximation, in which state equations are evaluated at the middle of the nodes. This method results in control histories that are piecewise constant and states that are piecewise linear. Constraints on control rates are enforced by a forward difference scheme over all nodes. Equally spaced nodes are used. The resulting parameter optimization problems are solved with the software program NPSOL.[29] In the results presented hereafter, analytical gradient expressions are provided for the objective functions, whereas gradients for the nonlinear constraints are calculated numerically.

Strictly speaking, optimal trajectories obtained in this approach only represent approximations to solutions of the original problems. These approximations normally approach the original solutions as the number of nodes becomes large. On the other hand, a large number of nodes would require long computational times. Sensitivity studies were conducted on the number of nodes, and it was found that the use of 11–21 nodes offers a good compromise between accuracy and computational speed for problems in this paper. Results presented hereafter are obtained with 21 equally spaced nodes.

D. Initial Conditions for Optimal Control Problems

It is assumed that during the takeoff run, the nacelle is tilted forward to $i_n = 70$ deg, and the tiltrotor has a ground acceleration of $0.2\,g$ and a liftoff speed of $V_L = 40$ kn. Once in the air, the aircraft maintains its acceleration with a constant flight-path angle of $\gamma = 8$ deg until the engine failure occurs. These takeoff assumptions are consistent with the XV-15 short takeoffs described in Ref. 30.

A period of t_d seconds is assumed for the pilot delay, during which the rotor speed governor is on, the pilot's longitudinal stick is held constant, and the nacelle angle is fixed. The thrust coefficient C_T varies to maintain a constant rotor speed and is determined by the following feedback control law that represents the rotor speed governor control system:

$$\dot{\Omega} + K_\Omega(\Omega - \Omega_0) = 0 \tag{48}$$

An augmented steady-state analysis is conducted to determine the control functions at the point of engine failure. The equations of motion are then integrated with these control assumptions for the period of pilot delay, to produce initial conditions for the subsequent optimization of flight paths.

V. Optimal Trajectories with Speed Governor On or Off

During tiltrotor flights in OEI after the pilot delay, the rotor speed governor may remain active in attempts to keep the rotor speed constant, or it might be switched off so that rotor rotational kinetic energy can be used in a power shortage situation. Optimal trajectories in OEI with the speed governor on and off are now compared. For the following results, it is assumed that $W = 14{,}000$ lb and the pilot delay is $t_d = 1$ s. After 1 s, the pilot recognizes the engine failure and takes appropriate actions. When the rotor speed governor is turned off, the rotor speed is allowed to vary between $\bar{\Omega}_{\max} = 1.1$ and $\bar{\Omega}_{\min} = 0.78$. To simulate the use of active rotor speed governor, much tighter bounds on rotor speed variations are imposed, where $\bar{\Omega}_{\max} = 1.002$ and $\bar{\Omega}_{\min} = 0.998$.

A. CTO Flight

Figure 3 compares optimal trajectories of the transient CTO flight in OEI with the speed governor turned on and off. With the speed governor turned off, the rotor speed is decreased to increase thrust after the pilot recognition period. The nacelle angle decreases to help climb and to increase forward speed. Steady-state climbout is achieved at the end of the trajectory. Keeping rotor speed roughly constant, the thrust is increased slightly once the pilot recognizes the engine failure. The nacelle angle first increases and eventually decreases to help the climb. The power required stays very close to the power available because the rotor speed is only allowed to vary by a small percentage. In both cases, the body pitch angle increases.

As shown in Fig. 3, tiltrotor flight paths in CTO with the speed governor on are similar to those with varying rotor speed. This is because CTO flight is relatively easy and quick due to the moderate speeds attained while accelerating on the runway and at the nominal weight of 14,000 lb. Given the opportunity to trade rotor speed

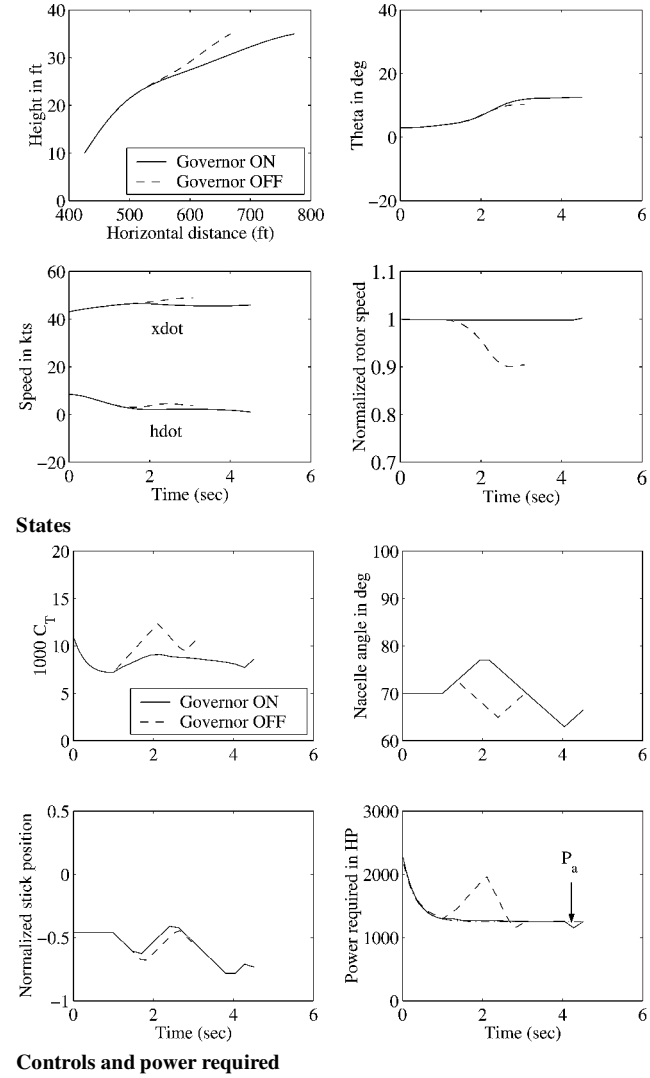

Fig. 3 CTO flight with rotor speed governor on and off.

for thrust, only 10% of the nominal rotor speed is used in the optimal maneuver. Correspondingly, in this example, using rotor speed energy decreases the runway length required by about 100 ft and decreases the time required to accomplish CTO after the delay by approximately 2 s.

B. RTO Flight

Figure 4 compares the optimal RTO trajectories in OEI with the speed governor turned on and off. With the speed governor turned off, the rotor speed is first increased after the pilot delay, as thrust and power required are decreased. The power required is then increased, accompanied by the decrease of rotor speed and the increase of thrust. The pitch angle and nacelle angle are raised to their maximum to reduce the forward speed. Pitch is then decreased to land safely. With the speed governor turned on, on the other hand, the tiltrotor pitches up and then down to maintain a reasonable forward speed, to keep the power required close to the power available to maintain a constant rotor speed. This is in part achieved by the nacelle angle movement. The pitch is finally recovered at the end. Thrust and power required are increased at the last moment for landing.

Optimal RTO flights with or without constant rotor speed are very different. With active rotor speed control, the tiltrotor takes 300 ft more to land back on the runway. It also touches down with a much greater forward speed and, therefore, needs even more space to decelerate on the runway. The total difference in runway lengths is almost 500 ft. This is because the RTO flight in OEI is inherently more difficult than the CTO flight. The moderate speed attained during the short takeoff ground run makes aborting the takeoff more difficult than continuing it. When allowing rotor speed to vary, the RTO rotor speed reaches both the maximum and the minimum limit during the flight.

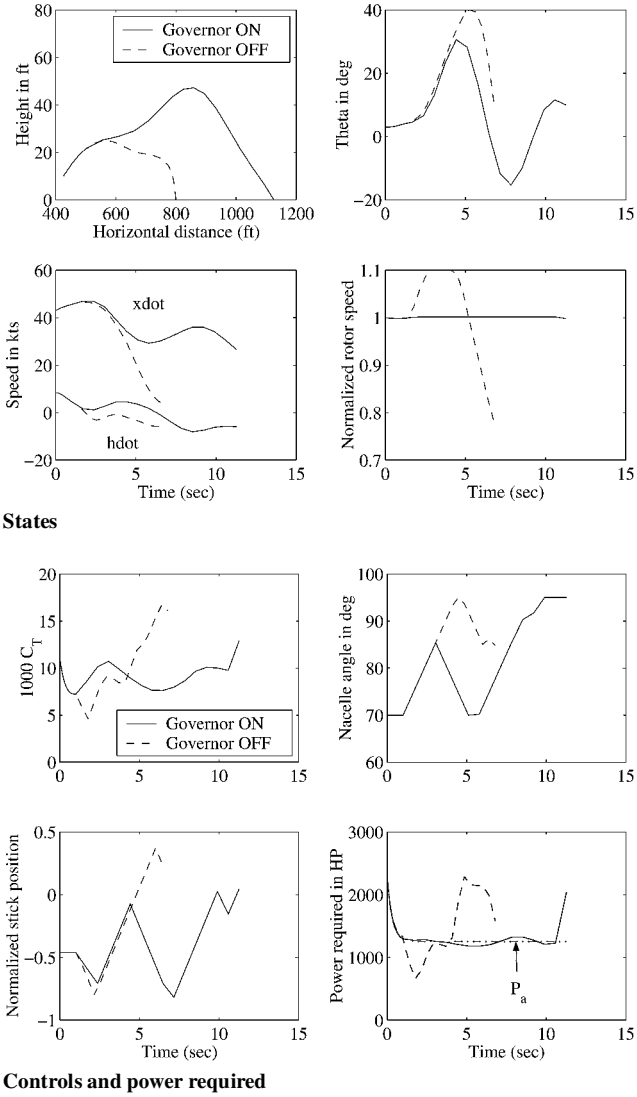

Fig. 4 RTO flight with rotor speed governor on and off.

Table 1 Runway lengths required with speed governor on and off

Governor	CTO, ft	RTO, ft
Off	667	802
On	773	1283

Table 2 Runway lengths required at different weights

Weight, lb	CTO, ft	RTO, ft
13,000	633	802
14,000	667	802
15,000	710	817

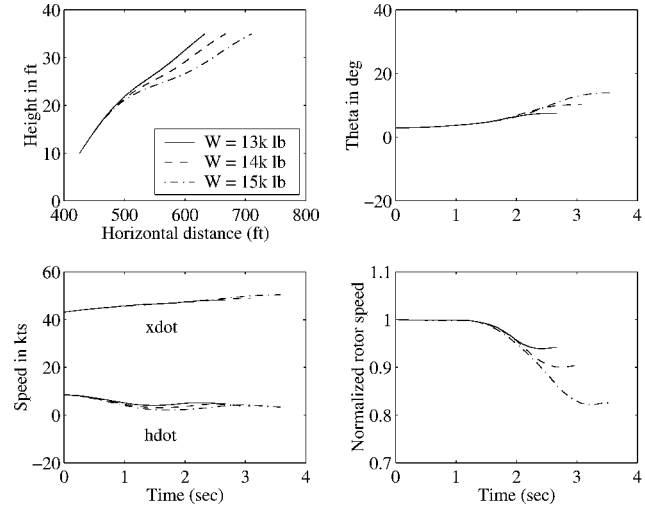

Fig. 5 CTO flights with different gross weights.

Table 1 shows a comparison of runway lengths required for this nominal 14,000-lb takeoff case. It shows that allowing the use of the rotor speed energy is significantly more optimal. This is especially true in the RTO case.

Note that, in practice, the potential benefits of using rotor speed energy might be outweighed by the risk of stalling the blades. Because tiltrotor blades are smaller than helicopter blades, their speed will change faster when using the rotor energy.

VI. Effects of Different Takeoff Conditions

Because the rotor speed governor-off case is found to be more optimal, this case is investigated further. This section systematically examines the effects of varying the takeoff assumptions.

A. Effects of Different Takeoff Weights

Figure 5 compares optimal CTO trajectories with three different gross weights: $W = 13{,}000$; 14,000; and 15,000 lb. As the gross weight increases, the transient CTO flight takes longer time, higher thrust, and results in a larger steady-state pitch angle. Also, more rotor speed is traded for thrust as the weight increases. In the case of rejected takeoff, as shown in Fig. 6, a larger gross weight results in less flight time and a larger forward speed at touchdown. The touchdown position is roughly constant with weight, though.

Table 2 compares runway lengths required for CTO and RTO at different gross weights. Runway lengths required for RTO flights are always significantly greater than those for CTO flights. If sufficient runway length is available, the tiltrotor aircraft can take off with the maximum gross weight of 15,000 lb even in the event of a single engine failure.

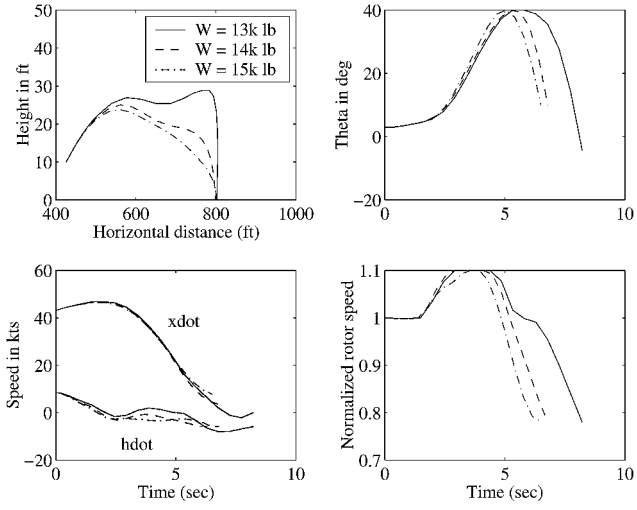

Fig. 6 RTO flights with different gross weights.

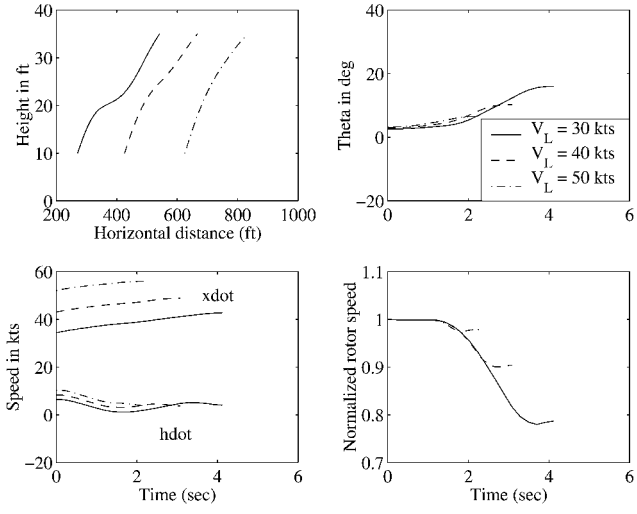

Fig. 7 CTO flights with different liftoff speeds.

B. Effects of Varying the Liftoff Speed

Figure 7 shows the effects of the liftoff speed V_L on the transient CTO flight in OEI. As the liftoff speed is increased, the runway length required for the ground acceleration is also increased. On the other hand, the rotor speed loss is smaller during the transient CTO flight with a larger liftoff speed. Because the rotor speed limit is reached, the case of $V_L = 30$ kn would probably have a difficult time carrying more weight. From a CTO point of view, lifting off at a slower speed shortens the required runway length, but it decreases the climbout capability in terms of possible gross weights.

Figure 8 shows the effects of the liftoff speed on the RTO flight in OEI. As the liftoff speed is increased, the total runway length required for RTO is greatly increased because it takes more runway length for the tiltrotor to accelerate to the liftoff speed and more runway length for the tiltrotor to decelerate to a stop. The maximum height of the flight path is also increased as the aircraft climbs to slow itself down. From an RTO point of view, lifting off at a slower speed shortens the required runway length.

Analyzing CTO and RTO together shows that the medium speed is the best compromise to keep the runway length small and still have good OEI climbout ability. Table 3 compares runway length requirements for CTO and RTO in OEI at different liftoff speeds.

C. Effects of Different Engine Failure Heights

Figure 9 shows the resulting optimal transient CTO flights for single engine failures occurring at different heights. With a lower engine failure height, the tiltrotor would take a longer time and use more rotor speed drop to achieve a steady OEI climbout. This is because the tiltrotor would have smaller speed and height at the point of engine failure and a longer distance to climbout. Figure 10 shows the effects of different engine failure heights on RTO flights. In a RTO, a lower engine failure height results in less flight time to touchdown. The touchdown speed in RTO is roughly constant despite variations in engine failure heights, but the runway length required increases as the engine failure height increases because of the higher speed at the engine failure point.

Table 4 shows runway length requirements for different engine failure heights. As the assumed engine failure height increases, the runway length required for CTO decreases slightly, whereas the runway length required for RTO increases.

Table 3 Runway lengths requirements for different liftoff speeds

V_L, kn	CTO, ft	RTO, ft
30	542	578
40	667	802
50	833	1142

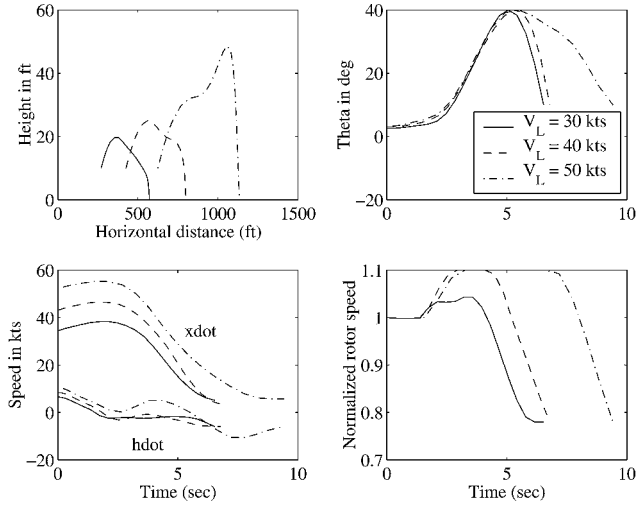

Fig. 8 RTO flights with different liftoff speeds.

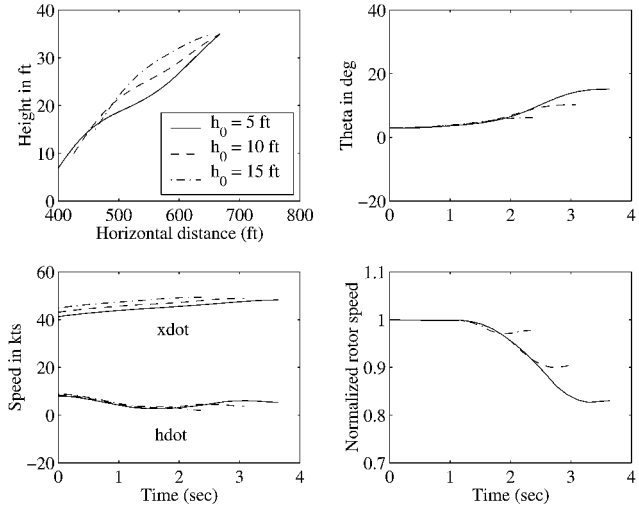

Fig. 9 CTO flights from different engine failure heights.

D. Other Systematic Studies

Effects of different takeoff flight-path angles and accelerations are also studied. Because of the limitation of space, details of these

Table 4 Runway lengths required for different failure heights

h_0, ft	CTO, ft	RTO, ft
5	668	746
10	667	802
15	665	867

Table 5 Runway lengths required at different takeoff angles

γ_0, deg	CTO, ft	RTO, ft
6	735	842
8	667	802
10	615	777

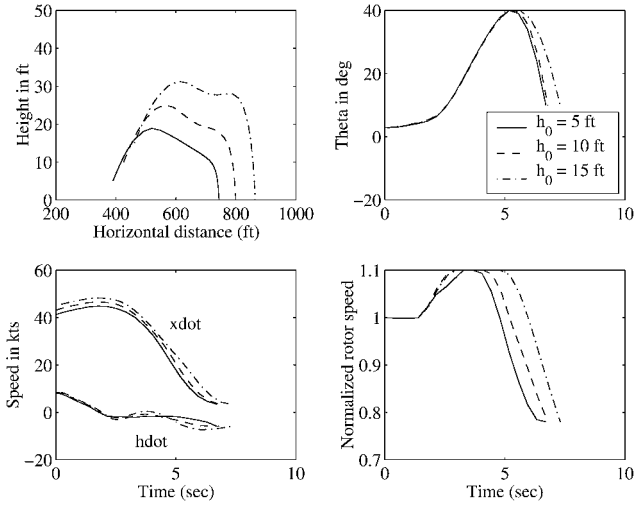

Fig. 10 RTO flights from different engine failure heights.

comparisons are omitted. Main results of these comparison studies are summarized hereafter.

For CTO flights in OEI, the runway length required decreases along with thrust and power required as the takeoff flight-path angle increases. This is because increasing the takeoff angle increases the initial vertical speed and decreases the horizontal speed. Flight time and pitch angle required also decrease with increased takeoff angle. Greater takeoff angles require more initial power. Therefore, the maximum takeoff angle possible is limited by the maximum takeoff power available and the gross weight. For RTO flights in OEI, the runway length required decreases as the takeoff angle increases. This is again because increasing the takeoff angle increases the vertical speed and decreases the horizontal speed. The RTO flights are almost identical for different takeoff angles, except that an increase in the takeoff angle corresponds to a decrease in the required runway length. CTO and RTO results viewed together indicate that a high takeoff angle should be used for which there is enough power available for the given takeoff weight. Table 5 presents corresponding runway lengths required.

Effects of takeoff accelerations before engine failure are also studied. For CTO flights, a higher acceleration gives a higher initial speed at engine failure. A reasonable level of acceleration would allow the tiltrotor to continue flight easily in the event of an engine failure. On the other hand, excessive accelerations, even if the power available permits, would result in a large momentum for the tiltrotor aircraft to continue in the nominal takeoff direction. In the event of an engine failure, this momentum would make it difficult for the aircraft to follow an optimal flight path in the transient CTO phase to reduce the runway required. Overall, the shortest CTO runway length is obtained for the middle acceleration of 0.2 g. For RTO flights, a higher acceleration also gives a higher speed at engine failure, but a shorter runway has been used when the RTO flight begins. Overall, a larger takeoff acceleration results in a shorter runway length required for the RTO flight in OEI. When this is looked at in conjunction with the CTO results, it indicates that either 0.2 g or 0.3 g acceleration is good. Table 6 compares the corresponding runway length requirements.

E. Optimal TDP Conditions

All results calculated and shown in Table 6 indicate that runway lengths required for RTO flights are longer than those for CTO. This is in part caused by the acceleration of tiltrotor aircraft to moderate speeds before engine failure. At these moderate speeds, OEI climbout is natural and takes less time than RTO. The overall runway length requirement is minimized by selecting takeoff decision point conditions that reduce the runway length required for rejected takeoff. Referring to Table 4, the TDP should be selected close to the liftoff condition: $h_{\mathrm{TDP}} = 0$. In other words, the takeoff flight should be continued if an engine failure occurs once the tiltrotor is off the runway.

VII. Sensitivity Analyses

Although the vertical plane rigid-body model provides a good description of the XV-15 aircraft, it is unavoidable that model uncertainties exist. Sensitivity analyses are now conducted to examine the effects of model uncertainties on optimal tiltrotor flight trajectories in OEI. In the following studies, the nominal case is assumed to have $W = 14{,}000$ lb and one engine failure occurs at the moment the aircraft is lifting off ($h_0 = 0$).

As shown in Table 7, the length of the pilot delay period is not vitally significant to tiltrotor OEI flight in a short takeoff operation. This is because in both the CTO and RTO flight in OEI, the tiltrotor moves favorably during the pilot delay period after the power loss. Specifically, the tiltrotor is still climbing, which is advantageous to CTO. It is also decelerating, which is favorable to RTO. In comparison, the length of pilot delay is critical to tiltrotor OEI flight in a vertical takeoff operation.[14]

Table 8 shows the effects of selected uncertain model parameters on runway length requirements during OEI flights. Overall, uncertainties in these parameters have small effects on the short takeoff performance.

The effects of control rate limits on the short takeoff performance are also studied. Sensitivity analysis shows that multiplying the

Table 6 Runway lengths required at different takeoff accelerations

a, g	CTO, ft	RTO, ft
0.1	1012	1123
0.2	667	802
0.3	692	721

Table 7 Effects of pilot delay on runway length requirements in OEI

Delay, s	CTO, ft	RTO, ft
0.5	611	647
1.0	665	689
2.0	770	786

Table 8 Effects of model uncertainties on runway lengths in OEI

Parameter	Value	CTO, ft	RTO, ft
All	Nominal values	665	689
K_{ind}	1.20	698	710
(1.10 nominal)	1.05	653	681
c_d	0.02	715	702
(0.015 nominal)	0.01	630	681
η_p	0.9	701	699
(0.95 nominal)	1.0	640	682

nominal rate limits by two or dividing by five has small effects, except that the CTO runway length would become very large for the smallest control rate limits.

VIII. Conclusions

This paper studies optimal tiltrotor aircraft flight paths and performance limits in the event of a single engine failure during a short takeoff operation. A longitudinal rigid-body model is developed. Tabular aerodynamic data from the XV-15 tiltrotor aircraft are fit to smooth functions. Flights after an engine failure are formulated as nonlinear optimal control problems, and a direct approach using collocation and nonlinear programming is employed to obtain numerical solutions. To determine initial flight conditions from the short takeoff procedure, an augmented steady-state analysis is conducted with constant accelerations, and pilot response delays are included. Both CTO and RTO after engine failure are studied, and the effect of an active rotor speed governor on optimal flight paths is examined. Sensitivity analyses are conducted on the short takeoff procedure and model uncertainties for the case when the rotor speed governor is switched off.

To minimize the overall required runway length, the TDP should be close to the tiltrotor liftoff point for the short takeoff operation. Continued takeoffs are found to be easy for large gross weights in OEI with a relatively low OEI power rating, regardless of whether the rotor speed governor is active or switched off. On the other hand, rejected takeoffs are found to always require longer runway lengths than continued takeoffs. This is especially true when the rotor speed governor remains active. Overall, the tiltrotor would require shorter runway lengths for safe CTO and RTO flights with the rotor speed governor turned off. The tiltrotor aircraft is found to be able to carry the maximum gross weight in the presence of one engine failure. Sensitivity analyses indicate that in general, model uncertainties have small effects on tiltrotor short takeoff OEI performance.

Appendix A: Aerodynamic Forces and Moments

Aerodynamic forces and moments are determined from contributions of the fuselage, the wing–pylon system, and the horizontal stabilizer, as follows:

$$A_z = -L_f \cos\alpha_f - D_f \sin\alpha_f - L_{w_{\text{fs}}} \cos\alpha_{w_{\text{fs}}} - D_{w_{\text{fs}}} \sin\alpha_{w_{\text{fs}}} - L_{w_{\text{ss}}} \cos\alpha_{w_{\text{ss}}} - D_{w_{\text{ss}}} \sin\alpha_{w_{\text{ss}}} - L_{\text{hs}} \cos\alpha_{\text{hs}} \tag{A1}$$

$$A_x = L_f \sin\alpha_f - D_f \cos\alpha_f + L_{w_{\text{fs}}} \sin\alpha_{w_{\text{fs}}} - D_{w_{\text{fs}}} \cos\alpha_{w_{\text{fs}}} + L_{w_{\text{ss}}} \sin\alpha_{w_{\text{ss}}} - D_{w_{\text{ss}}} \cos\alpha_{w_{\text{ss}}} + L_{\text{hs}} \sin\alpha_{\text{hs}} \tag{A2}$$

$$M = M_{a_f} - l_F(L_f \cos\alpha_f + D_f \sin\alpha_f) - h_F(L_f \sin\alpha_f - D_f \cos\alpha_f) + M_{a_w} - l_W\left(L_{w_{\text{fs}}} \cos\alpha_{w_{\text{fs}}} + D_{w_{\text{fs}}} \sin\alpha_{w_{\text{fs}}} + L_{w_{\text{ss}}} \cos\alpha_{w_{\text{ss}}} + D_{w_{\text{ss}}} \sin\alpha_{w_{\text{ss}}}\right) - h_W\left(L_{w_{\text{fs}}} \sin\alpha_{w_{\text{fs}}} - D_{w_{\text{fs}}} \cos\alpha_{w_{\text{fs}}} + L_{w_{\text{ss}}} \sin\alpha_{w_{\text{ss}}} - D_{w_{\text{ss}}} \cos\alpha_{w_{\text{ss}}}\right) - l_{\text{HS}} L_{\text{hs}} \cos\alpha_{\text{hs}} - h_{\text{HS}} L_{\text{hs}} \sin\alpha_{\text{hs}} \tag{A3}$$

where

$$L_f = q_f \bar{L}_f(\alpha_f) \tag{A4}$$

$$D_f = q_f \bar{D}_f(\alpha_f) \tag{A5}$$

$$M_{a_f} = q_f \bar{M}_{a_f}(\alpha_f) \tag{A6}$$

$$L_{w_{\text{fs}}} = q_{w_{\text{fs}}} S_{w_{\text{fs}}} C_{L_w}\left(\alpha_{w_{\text{fs}}}; \delta_{\text{fl}}, \mathcal{M}\right) \tag{A7}$$

$$D_{w_{\text{fs}}} = q_{w_{\text{fs}}} S_{w_{\text{fs}}} C_{D_w}\left(\alpha_{w_{\text{fs}}}; \delta_{\text{fl}}, \mathcal{M}\right) \tag{A8}$$

$$L_{w_{\text{ss}}} = q_{w_{\text{ss}}} S_{w_{\text{ss}}} C_{L_w}\left(\alpha_{w_{\text{ss}}}; \delta_{\text{fl}}, \mathcal{M}\right) \tag{A9}$$

$$D_{w_{\text{ss}}} = q_{w_{\text{ss}}} S_{w_{\text{ss}}} C_{D_w}\left(\alpha_{w_{\text{ss}}}; \delta_{\text{fl}}, \mathcal{M}\right) \tag{A10}$$

$$M_{a_w} = \left(q_{w_{\text{fs}}} S_{w_{\text{fs}}} + q_{w_{\text{ss}}} S_{w_{\text{ss}}}\right) c_w C_{M_{a_w}}(i_n; \delta_{\text{fl}}, \mathcal{M}) \tag{A11}$$

$$L_{\text{hs}} = q_{\text{hs}} S_{\text{hs}} C_{L_{\text{hs}}}(\alpha_{\text{hs}}, \delta_e) \tag{A12}$$

and

$$q_f = \frac{1}{2}\rho\left[(u - qh_F)^2 + (w + ql_F)^2\right] \tag{A13}$$

$$\alpha_f = \tan^{-1}\left(\frac{w + ql_F}{u - qh_F}\right) = \sin^{-1}\left(\frac{w + ql_F}{\sqrt{(u - qh_F)^2 + (w + ql_F)^2}}\right) \tag{A14}$$

$$q_{w_{\text{fs}}} = \frac{1}{2}\rho\left[(u - qh_W)^2 + (w + ql_W)^2\right] \tag{A15}$$

$$\alpha_{w_{\text{fs}}} = \tan^{-1}\left(\frac{w + ql_W}{u - qh_W}\right) + \alpha_{w_0} \tag{A16}$$

$$q_{w_{\text{ss}}} = \frac{1}{2}\rho\left\{[u - qh_W + \eta_i v_i \cos(i_n - \beta)]^2 + [w + ql_W - \eta_i v_i \sin(i_n - \beta)]^2\right\} \tag{A17}$$

$$\alpha_{w_{\text{ss}}} = \tan^{-1}\left(\frac{w + ql_W - \eta_i v_i \sin(i_n - \beta)}{u - qh_W + \eta_i v_i \cos(i_n - \beta)}\right) + \alpha_{w_0} \tag{A18}$$

$$q_{\text{hs}} = \frac{1}{2}\eta_h \rho\left[(u - qh_{\text{HS}})^2 + (w + ql_{\text{HS}})^2\right] \tag{A19}$$

$$\alpha_{\text{hs}} = \tan^{-1}\left(\frac{w + ql_{\text{HS}}}{u - qh_{\text{HS}}}\right) + \alpha_{\text{hs}_0} \tag{A20}$$

In the preceding expressions, $l_{(\,)}$ is the horizontal location of a specific aerodynamic center behind the center of gravity, and $h_{(\,)}$ is the vertical location above the center of gravity. The subscripts F, W, and HS represent the fuselage, the wing, and the horizontal stabilizer, respectively.

Because part of the wing is in the rotor slip stream and part is in the freestream, it experiences different flow velocities at its two different parts. As an approximation, the wing's contribution to the force and pitching moment is developed in two separate parts, one for the portion of the wing in the slip stream and one for the portion in the freestream. These are distinguished by the subscripts ss and fs, respectively. In this paper, a simplified equation dependent on nacelle angle and forward speed is developed to calculate areas of the wing under the slip-stream influence:

$$S_{w_{\text{ss}}} = S_{\text{ss}_{\max}}[\sin(ai_n) + \cos(bi_n)][(u_{\text{cr}} - u)/u_{\text{cr}}] \tag{A21}$$

where $S_{\text{ss}_{\max}} = 2\eta_{\text{ss}} R c_w$. $S_{w_{\text{ss}}} = 0$ for $i_n < 60$ deg or $u \geq u_{\text{cr}}$. In this paper, $u_{\text{cr}} = 40$ ft/s. Parameters a and b are chosen such that

$$\sin[a(\pi/2)] + \cos[b(\pi/2)] = 1$$

$$\sin[a(\pi/3)] + \cos[b(\pi/3)] = 0$$

and found numerically to be $a = 1.386$ and $b = 3.114$. Once the area of the wing under the slip-stream influence is determined,

$$S_{w_{\text{fs}}} = S_w - S_{w_{\text{ss}}} \tag{A22}$$

Appendix B: Aerodynamic Data and Optimization Parameters

Aerodynamic data and parameters of the XV-15 aircraft are given in Refs. 1–6 and 25. The following aerodynamic coefficients are needed to determine the aerodynamic forces and moments and are

fitted into smooth functions by Carlson[14] based on tabular data at incompressible flow conditions:

$$\bar{L}_f(\alpha_f) \triangleq L_f/q_f, \qquad \bar{D}_f(\alpha_f) \triangleq D_f/q_f$$

$$\bar{M}_{af}(\alpha_f) \triangleq M_{af}\big/q_f$$

and

$$C_{L_w}(\alpha_w, \delta_{\text{fl}}), \qquad C_{D_w}(\alpha_w, \delta_{\text{fl}}), \qquad C_{M_w}(i_n, \delta_{\text{fl}}), \qquad C_{L_{\text{hs}}}(\alpha_{\text{hs}}, \delta_e)$$

from which

$$C_{L_f} = \frac{L_f(\alpha_f)}{q_f S_w} = \frac{\bar{L}_f(\alpha_f)}{S_w}$$

$$C_{D_f} = \frac{D_f(\alpha_f)}{q_f S_w} = \frac{\bar{D}_f(\alpha_f)}{S_w}$$

$$C_{M_f} = \frac{M_f(\alpha_f)}{q_f S_w c_w} = \frac{\bar{M}_f(\alpha_f)}{S_w c_w}$$

The XV-15 aircraft has a design gross weight of 13,000 lb; a maximum gross weight of 15,000 lb; $R = 12.5$ ft; $\Omega_0 = 61.68$ rad/s; $i_{n,\max} = 95$ deg; $i_{n,\min} = 0$; and $\sigma = 0.089$. Nominal modeling parameters used in the optimizations are selected as follows: $P_{\text{OEI}} = 1250$ hp, $t_p = 0.2$ s, $t_d = 1.0$ s, $\theta_{\max} = 40$ deg, $\theta_{\min} = -40$ deg, $h_{\min} = 0$, $C_{T_{\max}} = 0.17\sigma$, $C_{T_{\min}} = 0.0001\sigma$, $K_{\text{ind}} = 1.15$, $f_G = 1.0$, $c_d = 0.015$, $\eta_{\text{ss}} = 0.9$, $\eta_i = 1.5$, $\eta_p = 0.95$, $\eta_h = 0.9$, $\beta_{\max} = 12$ deg, $\delta_{e_{\max}} = 20$ deg, $K_\Omega = 12$, and $(\dot{i}_n)_{\max} = 7.5$ deg/s. Control rate limitations are imposed as $(\mathrm{d}\bar{C}_T/\mathrm{d}\tau)_{\max} = 5.0$ and $(\mathrm{d}\bar{s}/\mathrm{d}\tau)_{\max} = 0.5$. With the rotor speed governor turned off, $\bar{\Omega}_{\max} = 1.1$ and $\bar{\Omega}_{\min} = 0.78$. With rotor speed governor turned on, $\bar{\Omega}_{\max} = 1.002$ and $\bar{\Omega}_{\min} = 0.998$. For RTOs, $\theta_{f,\min} = -5$ deg, $\theta_{f,\max} = 10$ deg, $i_{n_{f,\min}} = 60$ deg, $\dot{h}_{f,\max} = 10$ fps, and $\dot{x}_{f,\max} = 100$ fps. It is assumed that $\delta_{\text{fl}} = 20$ deg. Conversion factors are 1 kn = 0.5144 m/s, 1 ft = 0.3048 m, 1 lb = 4.4482 N, and 1 hp = 550 ft-lb/s = 754.7 W.

Acknowledgments

This work was supported by NASA Ames Research Center through a cooperative agreement under NCC2-809. We thank Robert Chen, Daniel Dugan, William Decker, and William Hindson for many helpful discussions, and thank an anonymous reviewer for many valuable comments.

References

[1]Maisel, M. D., "Tilt Rotor Research Aircraft Familiarization Document," NASA TM X-62, 407, Jan. 1975.

[2]Dugan, D. C., Erhart, R. G., and Schroers, L. G., "The XV-15 Tilt Rotor Research Aircraft," NASA TM 81244, Sept. 1980.

[3]Churchill, G. B., and Dugan, D. C., "Simulation of the XV-15 Tilt Rotor Research Aircraft," NASA TM 84222, March 1982.

[4]Marr, R. L., Willis, J. M., and Churchill, G. B., "Flight Control System Development for the XV-15 Tilt Rotor Aircraft," *Proceedings of the 32nd Annual Forum of the American Helicopter Society*, American Helicopter Society, Washington, DC, May 1976, pp. 1042-1–1042-13.

[5]Wernicke, K. C., "Performance and Safety Aspects of the XV-15 Tilt Rotor Research Aircraft," *Proceedings of the 33rd Annual Forum of the American Helicopter Society*, May 1977, pp. 77.33-14-1–77.33-14-9.l

[6]Dugan, D. C., "Designing the V-22 Tiltrotor: A Flight Test Pilot's Perspective," *Vertiflite*, Vol. 44, No. 3, 1998, pp. 32–36.

[7]Federal Aviation Administration, *Certification of Transport Category Rotorcraft*, Advisory Circular AC-29A, 1987.

[8]Okuno, Y., and Kawachi, K.,"Optimal Control of Tiltrotor Aircraft Following Power Failure," *Proceedings of the 17th European Rotorcraft Forum*, Paper 91-28, Sept. 1991.

[9]Okuno, Y., and Kawachi, K.,"Optimal Takeoff Procedures for a Transport Category Tiltrotor," *Journal of Aircraft*, Vol. 30, No. 3, 1993, pp. 291, 292.

[10]Cerbe, T., Reichert, G., and Schrage, D. P., "Short Takeoff Optimization for the XV-15 Tiltrotor Aircraft," *Proceedings of the 17th European Rotorcraft Forum*, Berlin, Germany, Sept. 1991.

[11]Pollack, M., Warburton, F., and Curtiss, H. C., "A Simulation Study of Tiltrotor Vertical Takeoff Procedures Using Conventional and Variable Diameter Rotor Systems," *Proceedings of the 17th European Rotorcraft Forum*, Paper 91-26, Berlin, Germany, Sept. 1991.

[12]Warburton, F., and Curtiss, H. C., "Evaluation of Tilt Rotor Aircraft Design Utilizing a Real-Time Interactive Simulation," *Proceedings of the 48th Annual Forum of the American Helicopter Society*, Washington, DC, May 1992.

[13]Carlson, E. B., Zhao, Y. J., and Chen, R. N., "Optimal Trajectories for Tiltrotor Aircraft in Total Power Failure," *Proceedings of the 54th Annual National Forum of the American Helicopter Society*, American Helicopter Society, Washington, DC, May 1998.

[14]Carlson, E. B., "Optimal Tiltrotor Aircraft Operations During Power Failure," Ph.D. Dissertation, Dept. of Aerospace Engineering and Mechanics, Univ. of Minnesota, Minneapolis, MN, July 1999.

[15]Johnson, W., "Helicopter Optimal Descent and Landing After Power Loss," NASA TM 73244, May 1977.

[16]Lee, A. Y., Bryson, A. E., and Hindson, W. S., "Optimal Landing of a Helicopter in Autorotation," *Journal of Guidance, Control, and Dynamics*, Vol. 11, No. 1, 1988, pp. 7–12.

[17]Okuno, Y., Kawachi, K., Azuma, A., and Saito, A., "Analytical Prediction of Height-Velocity Diagram of a Helicopter Using Optimal Control Theory," *Journal of Guidance, Control, and Dynamics*, Vol. 14, No. 2, 1991, pp. 453–459.

[18]Okuno, Y., and Kawachi, K.,"Optimal Takeoff of a Helicopter for Category A STOL/ VTOL Operations," *Journal of Aircraft*, Vol. 30, No. 2, 1993, pp. 235–240.

[19]Schmitz, F., "Optimal Takeoff Trajectories of a Heavily Loaded Helicopter," *Journal of Aircraft*, Vol. 8, Nov. 9, 1971, pp. 717–723.

[20]Zhao, Y., and Chen, R. T. N., "Critical Considerations for Helicopters During Runway Takeoffs," *Journal of Aircraft*, Vol. 32, No. 4, 1995, pp. 773–781.

[21]Zhao, Y., Jhemi, A., and Chen, R. T. N., "Optimal VTOL Helicopter Operation in One Engine Failure," *Journal of Aircraft*, Vol. 33, No. 2, 1996, pp. 337–346.

[22]Gessow, A., and Myers, G. C., Jr., *Aerodynamics of the Helicopter*, Frederick Ungar, New York, 1952, Chap. 2.

[23]Stepniewski, W. Z., and Keys, C. N., *Rotary-Wing Aerodynamics*, Dover Publ., New York, 1984, Chap. 2.

[24]Johnson, W., *Helicopter Theory*, Princeton Univ. Press, Princeton, NJ, 1980, pp. 282, 283.

[25]Ferguson, S. W., "A Mathematical Model for Real Time Flight Simulation of a Generic Tilt-Rotor Aircraft," NASA CR-166536, 1988.

[26]Seywald, H., *Computational Optimal Control*, AIAA Short Course Notes, AIAA, San Diego, CA, July 29– 31, Pt. 4, 1996.

[27]Hull, D., "Conversion of Optimal Control Problems into Parameter Optimization Problems," AIAA Paper 96-3812, July 1996.

[28]Betts, J., "Survey of Numerical Methods for Trajectory Optimization," *Journal of Guidance, Control, and Dynamics*, Vol. 21, No. 2, 1998, pp. 193–207.

[29]Gill, P. E., Murray, W., Saunders, M. A., and Wright, M. H., "User's Guide for NPSOL (Version 4.0): A Fortran Package for Nonlinear Programming," Dept. of Operations Research, TR SOL 86-2, Stanford Univ., Stanford, CA, Jan. 1986.

[30]Weiberg, J. A., Dugan, D. C., and Gerdes, M. R., "XV-15 N703 Takeoff Performance," NASA Memo FHT: 237-5/4554, Sept. 1982.